Int. J. Heat Mass Transfer. Vol. 6, pp. 727–738. Pergamon Press 1963. Printed in Great Britain.

THE EFFECT OF TRANSVERSE MASS FLOW ON HEAT TRANSFER AND FRICTION DRAG IN A TURBULENT FLOW OF COMPRESSIBLE GAS ALONG AN ARBITRARILY SHAPED SURFACE

P. N. ROMANENKO and V. N. KHARCHENKO

Moscow State Timber Institute, Moscow, U.S.S.R.

(*Received* 10 *November* 1962)

Аннотация—Проведены экспериментальные исследования сопротивления и теплообмена при обтекании нагретым воздухом пористой поверхности при $dp/dx = 0$ и $dp/dx \neq 0$ и вдуве в турбулентный пограничный слой различных газов (гелия, воздуха, углекислого газа и фреона-12). Установлено влияние на сопротивление и теплообмен относительного расхода вдуваемых газов на плоской пластине, а в случае течения воздуха при $dp/dx \neq 0$, кроме того, и продольного градиента давления. Показано, что с ростом молекулярного веса вдуваемых газов их влияние на сопротивление и теплообмен уменьшается. Продольный градиент давления оказывает весьма существенное влияние на сопротивление трения.

Обработка опытных данных и обобщение результатов в виде зависимостей между безразмерными формпараметрами трения, градиента давления и вдува позволили установить связь между основными определяющими величинами, характеризующими турбулентный пограничный слой в условиях тепло- и массопереноса и продольного градиента давления.

NOMENCLATURE

x, y, co-ordinates;
u, v, components of flow velocity;
$\omega = u/u_1$, relative velocity;
p, pressure;
h, difference of levels in differential pressure gauge;
γ_h, specific weight of liquid in differential pressure gauge;
T, temperature (dependent variable);
T^*, stagnation temperature;
T_e, equilibrium temperature;
T_2, temperature of injected gas before porous plate;
$\bar{T}_w = T_w/T_1$, temperature factor;
R, gas constant;
z', weight concentration of the gas being injected into boundary layer;
ρ, density;
ν, kinematic viscosity;
c_p, (weight) heat capacity;
τ, tangential stress;
c_f, dimensionless friction factor;
l, mixing length;
$\varkappa, \beta$, empirical constants of turbulent flow;
δ, thickness of dynamic boundary layer;
$\xi = y/\delta$, dimensionless transverse co-ordinate;
$\delta^* = \int_0^\delta \left(1 - \frac{\rho u}{\rho_1 u_1}\right) dy$, attenuation thickness;
$\theta = \int_0^\delta \frac{\rho u}{\rho_1 u_1}\left(1 - \frac{\rho u}{\rho_1 u_1}\right) dy$, momentum loss
$\varphi = \int_0^{\delta_T} \frac{\rho u}{\rho_1 u_1}\left(\frac{T_1^* - T^*}{T_e - T_w}\right) dy$, depth of energy loss;
$H = \delta^*/\theta$, form parameter of boundary layer;

Re_L, Reynolds number (subscript refers to characteristic length chosen);

Pr, Prandtl number;

Sc, Schmidt number;

St, Stanton number;

$$b = \frac{\rho_w v_w}{\rho_1 u_1} \frac{2}{c_{f_0}}, \quad b_1 = \frac{\rho_w v_w}{\rho_1 u_1} \frac{2}{c_f}, \quad J = \frac{\rho_w v_w}{\rho_1 u_1} Re_\theta^{0.25} \quad \text{parameters of wall penetration;}$$

$$b_T = \frac{c_{pw} \rho_w v_w}{c_{p1} \rho_1 u_1} \frac{1}{St_0}, \quad b_{T1} = \frac{c_{pw} \rho_w v_w}{c_{p1} \rho_1 u_1} \frac{1}{St} \quad \text{thermal parameters of wall penetration;}$$

Γ, form parameter of longitudinal pressure gradient;

ζ, form parameter of drag.

Subscripts

1, parameters on external boundary of the boundary layer;

w, parameters on the wall;

o, parameters on impenetrable flat plate with isothermal flow;

$'$, parameters of injected gas into the boundary layer.

1. INTRODUCTION

One of the best methods of protecting surfaces in a stream from high temperature or kinetic energy effects, is to supply liquid or gas coolants through a porous wall.

The turbulent boundary layer has the greatest interest for industry since this layer predominates in situations which require porous cooling. Therefore, the problem of heat transfer and friction drag between a body and a parallel gas flow consists in obtaining methods for predicting heat transfer and drag coefficients of a turbulent boundary layer. Analytical solution is impossible at present since the physical mechanism of turbulent flow is not fully elucidated and the system of equations governing transfer of heat and momentum in a turbulent boundary layer is not implicit.

Various analytical methods have been developed based on a schematic representation of actual flow conditions and the introduction of great amount of doubtful approximations, and also on using additional experimental data [1–8]. Experimental results of the effect of air injection into a turbulent boundary layer on a flat plate on heat transfer and friction drag are reported by several workers [9–14]. They show that coefficients of heat transfer and friction drag decrease with increase in the rate of injected air.

A brief review of work on porous cooling is given in [15].

The effect of transverse gas flow injected into an incompressible liquid stream with negative pressure gradient is considered in [16]. Up till the present, however, no work is available on the effect of transverse mass flow on heat transfer with gradient gas flow.

In the present work the results are given for the drag and heat transfer with injection of air, helium, carbon dioxide and freon-12 into a turbulent boundary layer of heated air on porous plate with non-gradient and gradient flow.

2. EXPERIMENTAL RIG VARIABLES MEASURED AND MEASURING INSTRUMENTS

The experiments were carried out in the test section (Fig. 1). This section was a rectangular insulated duct. A copper porous plate 300 × 60 × 6 mm with 50 per cent porosity was fixed into the base of the duct. The side walls of the duct were movable, so that various longitudinal pressure gradients could be generated. The extreme divergence and convergence angles were 10° and 15°, respectively. The length of the test section was 420 mm, the entrance section was 150 × 80 mm.

Gases were forced through the porous plate by excess pressure which was generated in the bottom tank below the plate.

The air was injected into the tank from the receiver of an air compressor and the other gases were supplied from the cylinders through reduction valves. Statistic pressure drops on the plate were controlled by differential mercury pressure gauge. The flow rate of injected gas was determined from a calibration graph drawn up before the experiments at the known temperature of the plate and pressure on it. These

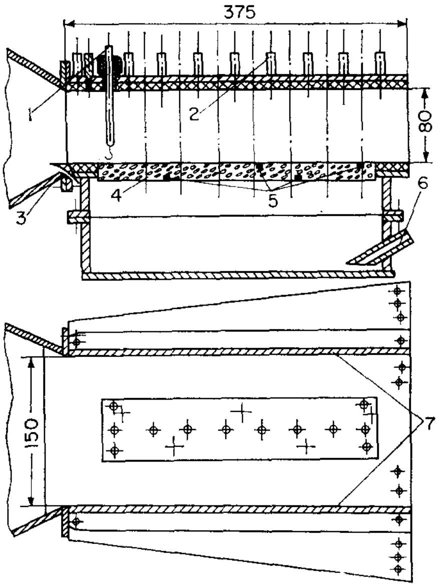

FIG. 1. Schematic drawing of test section. 1—temperature element and dynamic head transmitter; 2—static pressure transmitter; 3—suction of boundary layer; 4—porous plate; 5—thermocouple for measuring temperature on the plate; 6—supply of injected gas; 7—side walls.

graphs show the effect of volumetric permeability of the gas of interest through the plate on the pressure drop of various plate temperatures. Under the prescribed conditions volumetric permeability was determined on a special calibration unit by the volume of water ejected from the measuring tank by the gas forced through the plate. The porous plate was calibrated before the experiment and after it.

The test section was a part of the unit described in work [17].

In the experiment the following values were measured: air pressure and temperature at the exit of the heater (in front of the nozzle); dynamic pressure and the temperature of the air stream in seven cross sections over the length of the plate; the temperature of the plate at five points on the internal surface and at five points on the external one; the temperature of the injected gas in front of the plate; static pressure at ten cross sections along the plate.

Dynamic pressures in the boundary layer and in the non-disturbed flow of the reference cross section were measured by pneumatic measuring total pressure microtubes connected with differential pressure gauges filled with water or ethyl alcohol. Stream temperatures were measured by movable chromel-alumel thermocouples in the same cross sections of the test section where dynamic pressures were measured. Air temperatures in all the cross sections of the test section were recorded by an electronic balance potentiometer.

Pitot microtubes and microthermocouples were placed along the centre-line of the plate by means of traversing equipment which allowed measurement of dynamic pressures and temperatures in the cross sections every 0·05 mm. Simultaneously, in the first and the last cross sections dynamic pressure and temperature distributions were measured at the edges of the plate. These measurements showed that flow parameters were uniformly distributed through the width of the test section. Temperatures of the plate as well as those of the gas being injected were measured by chromel-alumel thermocouples and recorded by a portable potentiometer.

To ensure development the boundary layer over the starting portion of the porous plate, the boundary layer was sucked at a distance of 15 mm before the plate.

Before the experiments the plate was heated to a given temperature which was maintained constant during the experiments. The required temperature of the plate for every particular run was determined according to preliminary injections.

The experiments were carried out over the range of Re from 10^5 to 5×10^5. Injection rate $(\rho_w v_w)/(\rho_1 u_1)$ was measured from 0·0001 to 0·007, the flow temperature from 450 to 550°K, and the plate temperature from 375° to 420°K. Potential flow velocities were measured from 25 to 75 m/s.

3. INTERPRETATION OF DATA

Based on the measurement of dynamic and static pressures as well as of the flow temperatures at the reference cross sections of the boundary layer, and of the plate temperatures, distribution of the velocities and temperatures of the flow for every cross section were plotted. Integral parameters of the boundary layer δ^*,

θ, φ were determined from these plots. Then, changes of these parameters over the length of the test section were plotted (along the x-axis). Besides, changes of p, u, were plotted over the length of the section. All these data were used to estimate the drag coefficient c_f and the heat flux q_w on the porous plate from integral momentum and energy relations for the boundary layer.

For determining the flow velocity in the boundary layer the following original equation was used

$$u = \sqrt{\left(2h\frac{\gamma h}{\rho_1}\frac{\rho_1}{\rho}\right)}. \tag{1}$$

With air being injected, ρ was determined from the state equation $p = \rho gRT$ by the measured p in the cross section of interest and temperature T in a particular point of the boundary layer.

To determine the mixture density ρ when He, CO_2 and freon-12 are blown, the following relations were used.

In [11] it is shown that in case of a turbulent flow around a flat porous plate, it may be assumed

$$\frac{z'_w - z'}{z'_w} \approx \omega. \tag{2}$$

The gas constant R of the mixture was determined by the formula

$$R = z'R' + (1 - z')R_1$$
$$= z'_w(1 - \omega)(R' - R_1) + R_1 \tag{3}$$

hence

$$\frac{R}{R_1} = z'_w(1 - \omega)\left(\frac{R'}{R_1} - 1\right) + 1. \tag{4}$$

As is known

$$\frac{\rho_1}{\rho} = \frac{R}{R_1}\frac{T}{T_1} \tag{5}$$

then

$$\frac{\rho_1}{\rho} = \left[z'_w(1 - \omega)\left(\frac{R'}{R_1} - 1\right) + 1\right]\frac{T}{T_1}. \tag{6}$$

On substituting ρ_1/ρ from equation (6) into equation (1) we obtain the second power equation with respect to the velocity u.

$$u^2 - 2Qu + S = 0 \tag{7}$$

where

$$Q = \frac{\gamma h z'_w}{\rho_1 u_1 T_1}\left(1 - \frac{R'}{R_1}\right)T \,.\, h$$

$$S = \frac{\gamma h}{\rho_1 u_1}\left[z'_w\left(1 - \frac{R'}{R_1}\right) - 1\right]T \,.\, h.$$

From equation (7) a calculation formula is obtained for determination of the velocity through the cross section of the boundary layer.

Condition of constant air supply on the wall is expressed by equation (8)

$$\rho_w v_w = z'_w \rho_w v_w - D_w \rho_w (\mathrm{d}z'/\mathrm{d}y)_w. \tag{8}$$

Accounting for equation (2) and assuming $Sc = 1$, we obtain from equation (8) the formula for determination of the concentration of injected gas on the wall

$$z'_w = \frac{b_1}{1 + b_1} \tag{9}$$

The parameter of the permeability of the wall b_1 was estimated by the formula when the injection rate was known $(\rho_w v_w)/\rho_1 u_1)$

$$b_1 = \frac{\rho_w v_w}{\rho_1 u_1 St Pr^{2/3}}. \tag{10}$$

The Stanton number was determined by two independent methods:

1. From the heat balance equation

$$St = \frac{\rho_w v_w c_{pw}(T_w - T_2)}{\rho_1 u_1 c_{p1}(T_2 - T_w)}. \tag{11}$$

2. From the integral energy relation

$$\frac{\mathrm{d}\varphi}{\mathrm{d}x} + \frac{\varphi}{u_1}\frac{\mathrm{d}u}{\mathrm{d}x} - \frac{c_{pw}\rho_w v_w}{c_{p1}\rho_1 u_1} = St. \tag{12}$$

Local values of drag coefficient were also determined by two independent methods.

In the first case an integral momentum equation was used

$$\frac{\mathrm{d}\theta}{\mathrm{d}x} + \frac{\theta}{u_1}(H + 2)\frac{\mathrm{d}u_1}{\mathrm{d}x} - \frac{\rho_w v_w}{\rho_1 u_1} = \frac{c_f}{2}. \tag{13}$$

The second method was based on the experimental fact that in the great portion of the turbulent core of the boundary layer the logarithmic law for velocity distribution is valid.

Assume the Prandtl hypothesis of the mixing length

$$l = \varkappa y. \tag{14}$$

The total shear stress near the wall, as is shown in [3] may be expressed by

$$\tau_w = \rho l^2 \left(\frac{du}{dy}\right)^2 - \rho_w v_w u = \rho \varkappa^2 y^2 \left(\frac{du}{dy}\right)^2 - \rho_w v_w u. \tag{15}$$

By analogy with turbulent boundary layer on an impenetrable wall, introduce dynamic velocity of skin friction with injection of gas

$$v_{*w} = \sqrt{\left(\frac{\tau_w + \rho_w v_w u}{\rho}\right)} = u_1 \sqrt{\left[\left(\frac{c_f}{2} + \frac{\rho_w v_w}{\rho_1 u_1}\omega\right)\frac{\rho_1}{\rho}\right]}. \tag{16}$$

Then equation (15) is reduced to

$$v_{*w}^2 = \varkappa^2 y^2 \left(\frac{du}{dy}\right)^2 \tag{17}$$

or

$$\frac{\varkappa}{v_{*w}}\, du = \frac{dy}{y}. \tag{18}$$

Further, our problem is to determine the law of ρ_1/ρ distribution through the cross section of the boundary layer for various cases of gas blowing and to integrate equation (18).

When gas blowing is isothermal and when this gas is the same as that of the main flow, $\rho_1/\rho = 1$, consequently

$$v_{*w} = u_1 \sqrt{\left(\frac{c_f}{2} + \frac{\rho_w}{\rho_1}\frac{v_w}{u_1}\omega\right)} \tag{19}$$

and the integral of equation (18) taking into account equation (19) will be

$$2\varkappa \frac{\rho_1 u_1}{\rho_w v_w} \sqrt{\left(\frac{c_f}{2} + \frac{\rho_w v_w}{\rho_1 u_1}\omega\right)} = \ln y + C. \tag{20}$$

The constant of integration is determined from the condition that $u = 0$ at a certain distance from the wall y_0 which should be proportional to the length ν/v_* because of convenience of dimensions, i.e. $y_0 = \beta(\nu/v_*)$. Formula for the velocity profile will be in this case

$$2\varkappa \frac{\rho_1 u_1}{\rho_w v_w}\left[\sqrt{\left(\frac{c_f}{2} + \frac{\rho_w v_w}{\rho_1 u_1}\omega\right)} - \sqrt{\left(\frac{c_f}{2}\right)}\right] = \ln\left[\frac{Re_y \sqrt{(c_f/2)}}{\beta}\right]. \tag{21}$$

When homogeneous gas is non-isothermally injected into a region near the wall we assume similarity of velocities and temperatures

$$\frac{T - T_w}{T_1 - T_w} \approx \omega. \tag{22}$$

Then

$$\frac{T}{T_1} = \omega(1 - \bar{T}_w) + T_w. \tag{23}$$

However, since $(\rho_1/\rho) = (T/T_1)$, then

$$v_{*w} = u_1 \sqrt{\left\{\frac{c_f}{2} + \frac{\rho_w v_w}{\rho_1 u_1}\omega[\omega(1 - \bar{T}_w) + \bar{T}_w]\right\}}. \tag{24}$$

Keeping in mind the considerations used in deriving equation (21) we obtain

$$\frac{\varkappa}{\sqrt{L}} \ln \frac{2\sqrt{[L(L\omega^2 + M\omega + N)]} + 2L\omega + M}{2\sqrt{(LN)} + M} = \ln\left\{Re_y \frac{\sqrt{[(c_f/2) + M\omega + N]}}{\beta}\right\}. \tag{25}$$

Here for convenience assume

$$L = \frac{\rho_w v_w}{\rho_1 u_1}(1 - \bar{T}_w);\; M = \frac{c_f}{2}(1 - \bar{T}_w) + \frac{\rho_w v_w}{\rho_1 u_1}\bar{T}_w;\; N = \frac{c_f}{2}\bar{T}_w.$$

When a different gas is injected into a boundary layer, one can use the expression obtained above for ρ_1/ρ (16). The friction velocity in this case will be

$$v_{*w} = u_1 \sqrt{\left\{\left(\frac{c_f}{2} + \frac{\rho_w v_w}{\rho_1 u_1}\omega\right)\left[z'_w(1 - \omega)\left(\frac{R'}{R_1} - 1\right) + 1\right]\right\}} \tag{26}$$

for isothermal case,

$$v_{*w} = u_1 \sqrt{\left\{\left(\frac{c_f}{2} + \frac{\rho_w v_w}{\rho_1 u_1}\omega\right) \left[z_w'(1-\omega)\left(\frac{R'}{R_1} - 1\right) + 1\right][\omega(1-\bar{T}_w) + \bar{T}_w]\right\}} \quad (27)$$

for non-isothermal case.

Equation (25) will be the integral of equation (18) when foreign gas injection is isothermal, at $R' < R_1$ and coefficients in this case

$$L = z_w'\left(1 - \frac{R'}{R_1}\right)\frac{\rho_w v_w}{\rho_1 u_1};$$

$$M = \frac{\rho_w v_w}{\rho_1 u_1} + z_w'\left(1 - \frac{R'}{R_1}\right)\left(\frac{c_f}{2} - \frac{\rho_w v_w}{\rho_1 u_1}\right);$$

$$N = \frac{c_f}{2}\left[1 - z_w'\left(1 - \frac{R'}{R_1}\right)\right].$$

For a non-isothermal case integration of equation (18) at $R' < R_1$ is rather cumbersome. It may be simplified, however, to equation (25) by numerical estimation of its terms (when freon-12 and carbon dioxide are injected at $(\rho_w v_w)/(\rho_1 u_1) \approx 0{\cdot}01$, inaccuracy will be $\sim$1 per cent) and the coefficients

$$L = z_w'\left(1 - \frac{R'}{R_1}\right)\frac{\rho_w v_w}{\rho_1 u_1}\bar{T}_w + \frac{\rho_w v_w}{\rho_1 u_1}(1 - \bar{T}_w);$$

$$M = \frac{\rho_w v_w}{\rho_1 u_1}\bar{T}_w + z_w'\left(1 - \frac{R'}{R_1}\right)\left(\frac{c_f}{2} - \frac{\rho_w v_w}{\rho_1 u_1}\right)\bar{T}_w + \frac{c_f}{2}(1 - \bar{T}_w);$$

$$N = \frac{c_f}{2}\left[1 - z_w'\left(1 - \frac{R'}{R_1}\right)\right]\bar{T}_w.$$

Velocity profiles expressed by (21) and (25) in co-ordinates $\omega = f(\lg Re_y)$ are approximated with sufficient accuracy by straight lines.

Local drag coefficients are estimated in the following way: for the particular experimental conditions with known values of R'/R_1, $(\rho_w v_w)/(\rho_1 u_1)$ and $\bar{T}_w$ a grid of predicted velocity profiles is drawn for various values of c_f; then on this grid the experimentally obtained velocity profiles are superimposed and c_f is determined from its coincidence with one of the theoretical profiles.

4. FRICTION DRAG AND HEAT TRANSFER WITHOUT PRESSURE GRADIENT

Experimental data on the effect of transverse flow of air, helium and carbon dioxide on drag and heat transfer when a flat surface is in a turbulent flow of air without pressure gradient, are correlated graphically as

$$\left(\frac{c_f}{c_{f_0}}\right)_{Re_x} = f(b) \quad \text{and} \quad \left(\frac{St}{St_0}\right)_{Re_x} = f(b_T).$$

To determine c_{f0}, special experiments are carried out: a flat impenetrable wall was blown by an air stream at the wall temperature and at values of Re_x which prevailed in experiments with transverse injection of gases. Using the experimental data drag coefficient was determined from the integral momentum equation

$$\frac{c_{f_0}}{2} = \frac{d\theta_0}{dx} \quad (28)$$

Additionally, values of c_{f0} were determined by the Klauser method (19) and from the Blasius formula:

$$\frac{c_{f_0}}{2} = 0{\cdot}0296\, Re_x^{-0{\cdot}2}. \quad (29)$$

Experimental data on c_{f_0} obtained by equation (28) and using the Klauser method are in good agreement with those obtained from equation (29).

The Stanton number St_0 was determined by the following formula [18]:

$$St_0 = \frac{0{\cdot}0296\, Re_x^{-0{\cdot}2}}{1 + 0{\cdot}87\, A_1\, Re_x^{-0{\cdot}1}(Pr - 1)} \quad (30)$$

where $A_1 = 1{\cdot}5\, Pr^{-0{\cdot}167}$; Pr is the Prandtl number at the temperature of a non-disturbed stream.

In Fig. 2 the effect of air injection on the drag coefficient is shown. One can see that drag coefficient decreases with increase of the permeability parameter and at $b = 2$ it is 20 per cent of c_{f_0}. In the same figure the data of theoretical [3, 4, 8] and experimental [2, 13, 14] works are shown. The data of various investigators are essentially different; with increase in b, the general trend of c_f/c_{f_0} being to decrease with increase of b. The present authors' data agree

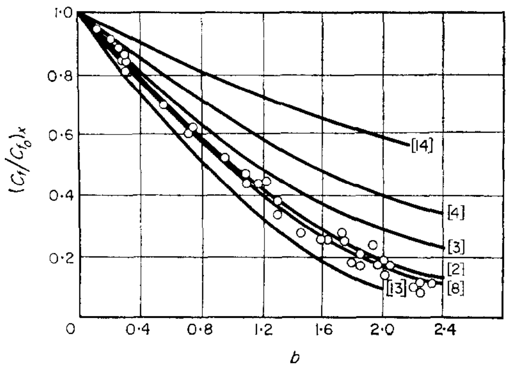

FIG. 2. The effect of injection rate on drag coefficient. Full lines refer to data of various authors.

well with the theoretical ones of [3] which is based on the Prandtl hypothesis on mixing length, and of [8] which uses limiting laws of friction drag. Experimental data of [2] obtained in conditions very similar to ours are in good agreement with the results of the present work. In [14] and [4] the results of injection effect on drag coefficient are underestimated, and in work [13] they are overestimated.

The effect of injection of gases with different molecular weights on drag coefficients is shown in Fig. 3. As should be expected, the greatest decrease of friction drag is observed with gases of low molecular weights. Freon-12 decreases friction drag less than air and especially helium. With equal gas flow rates, however, injection of helium is more effective compared with that of air than injection of air compared with that

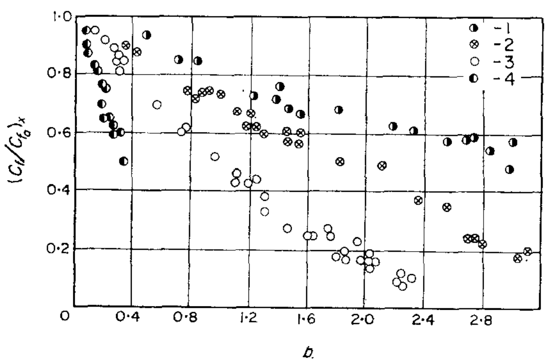

FIG. 3. The effect of injection rate of various gases on drag coefficient: 1—freon-12; 2—carbon dioxide; 3—air; 4—helium.

of freon-12. Carbon dioxide is intermediate between air and freon-12.

The effect of injection of gases with different molecular weights on heat transfer is illustrated in Fig. 4. The data of this plot show gas injection reduces considerably heat fluxes on the wall. That gases injected into the boundary layer with different molecular weights have almost the same effect on heat transfer as on friction drag is a characteristic feature. Helium which has very high heat capacity is a very effective coolant, whereas freon-12 (its heat capacity is smaller by a factor 8 than that of helium, other things being equal) diminishes heat

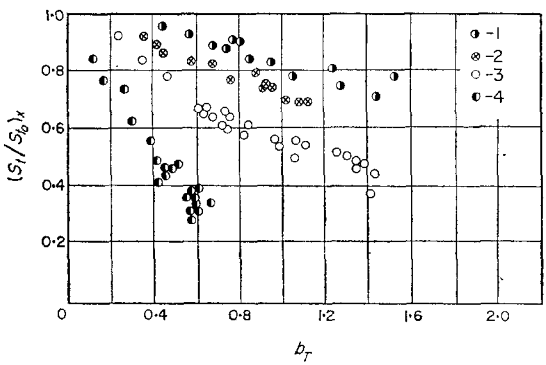

FIG. 4. The effect of injection rate of various gases on heat transfer coefficient: 1—freon-12; 2—carbon dioxide; 3—air; 4—helium.

transfer rate very little. Experimental points obtained on carbon dioxide and air with intermediate values of heat capacity lie between points for freon-12 and helium.

5. FRICTION DRAG AND HEAT TRANSFER OF A FLOW WITH PRESSURE GRADIENT

Experimental data on friction drag and heat transfer in a gradient flow of a porous wall are correlated by plotting relations between form parameters characterizing transfer of heat and momentum under the stream conditions considered.

The following form parameters are assumed for a dynamic turbulent boundary layer:

form parameter of pressure gradient

$$\Gamma = \frac{\theta}{u_1}\frac{du_1}{dx} Re_\theta^{0\cdot 25}, \tag{31}$$

form parameter of the friction law

$$\zeta = \frac{c_f}{2} Re_\theta^{0\cdot25}, \tag{32}$$

injection form parameter

$$J = \frac{\rho_w v_w}{\rho_1 u_1} Re_\theta^{0\cdot25}. \tag{33}$$

To establish the friction law for a turbulent boundary layer with longitudinal pressure gradient and transverse mass supply, the complex form parameter K is obtained, because of the following considerations.

In case of a laminar boundary layer the momentum equation on the wall will be of the form:

$$\rho_w v_w \left(\frac{\partial u}{\partial y}\right)_w = -\frac{dp}{dx} + \mu \left(\frac{\partial^2 u}{\partial y^2}\right)_w. \tag{34}$$

Let the velocity distribution u across the cross section of the boundary layer be a polynome of the fourth power, i.e.

$$\omega = f(\xi) = a + c\xi + d\xi^2 + e\xi^3 + f\xi^4. \tag{35}$$

To determine constants a, c, d, e, f boundary condition (34) should be satisfied and contact of curve (35) with the straight line $\omega = 1$ at $y = \delta$ should be of the second order

$$\omega = 1, \frac{\partial \omega}{\partial \xi} = 0, \frac{\partial^2 \omega}{\partial \xi^2} = 0 \text{ at } \xi = 1. \tag{36}$$

Introduce the dimensionless value

$$B = \frac{\left(\frac{\delta}{u_1}\frac{du_1}{dx} Re_\delta - 2\frac{\rho_w v_w}{\rho_1 u_1} Re_\delta\right)}{\left(\frac{1}{6}\frac{\rho_w v_w}{\rho_1 u_1} Re_\delta + 1\right)}. \tag{37}$$

The values of the coefficients of equation (35) are estimated as follows:

$$a = 0,\ c = 2 + \frac{B}{6},\ d = -\frac{B}{2},$$

$$e = -2 + \frac{B}{6},\ f = 1 - \frac{B}{6}. \tag{38}$$

Substituting these equations into equation (35) we obtain

$$\omega = F(\xi) + BG(\xi);$$

$$\left|\begin{array}{l} F(\xi) = 2(\xi) - 2\xi^3 + 3\xi^4 \\ G(\xi) = (1/6)(\xi - 3\xi^2 + 3\xi^3 - \xi^4) \end{array}\right]. \tag{39}$$

One can see from equation (39) that the velocity profiles give a variety of curves which depend on the form parameter B.

For a turbulent boundary layer a form parameter may be introduced which is similar in its structure to B, but in this case δ in equation (37) should be substituted for the thickness of momentum loss θ and Re for $Re^{0\cdot25}$, [20], i.e. the form parameter

$$K' = \frac{\left(\frac{\theta}{u_1}\frac{du_1}{dx} Re_\theta^{0\cdot25} - 2\frac{\rho_w v_w}{\rho_1 u_1} Re_\theta^{0\cdot25}\right)}{\left(\frac{1}{6}\frac{\rho_w v_w}{\rho_1 u_1} Re_\theta^{0\cdot25} + 1\right)}, \tag{40}$$

Over a wide range of blowing velocities

$$\frac{1}{6}\frac{\rho_w v_w}{\rho_1 u_1} Re_\theta^{0\cdot25} \ll \frac{1}{6}\frac{\rho_w v_w}{\rho_1 u_1} Re^{0\cdot25}$$

$$\approx 0\cdot015 \quad \text{at } \frac{\rho_w v_w}{\rho_1 u_1} = 0\cdot01.$$

Therefore it may be assumed

$$K \approx \frac{\theta}{u_1}\frac{du_1}{dx} Re_\theta^{0\cdot25} - 2\frac{\rho_w v_w}{\rho_1 u_1} Re_\theta^{0\cdot25}. \tag{41}$$

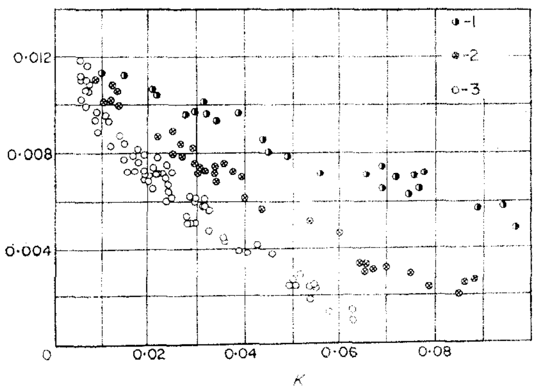

FIG. 5. The effect of injection rate of various gases and longitudinal pressure gradient on drag coefficient: 1—freon-12; 2—carbon dioxide; 3—air; 4—helium.

Correlation of the experimental data on friction drag with the relation $\zeta = f(K)$ shows that the form parameter K is actually an effective parameter for obtaining a relation between the drag coefficient, longitudinal pressure gradient and mass flow rate of the injected gas. In Fig. 5 a relation between ζ and K from our experimental data is shown. In plotting this relation the friction coefficient c_f in the form parameter ζ is defined taking into account heat tranfser correction $[2/\sqrt{(\bar{T}_w + 1)}]^2$.

If form parameters Γ, ζ and J are substituted into equation (13), it may be reduced to the following form

$$\frac{\mathrm{d}}{\mathrm{d}\bar{x}}(Re_\theta^{1\cdot 25}) = \{1\cdot 25[\zeta - (H+1)\Gamma + J]\}Re_L. \tag{42}$$

L is a characteristic linear dimension. Denote the expression in curly brackets of equation (42) by $F(\sigma)$ and determine the specific form of this function.

For a turbulent boundary layer with longitudinal pressure gradient on an impenetrable surface the expression in curly brackets of equation (42) is of the form $1\cdot 25[\zeta - (H + 1)\Gamma]$.

For a turbulent boundary layer on a flat penetrable plate this expression will be $1\cdot 25(\zeta + J)$.

According to our experimental data in Fig. 6 the function $1\cdot 25(\zeta + J)$ is plotted versus J for a turbulent boundary layer without pressure gradient when various gases are injected. This figure shows that $1\cdot 25(\zeta + J)$ is a linear function of J, but it has various angle coefficients depending on physical properties of injected gases.

$$F(J) = 1\cdot 25(\zeta + J) = 0\cdot 016 + mJ. \tag{43}$$

Values of the constant m in equation (43) for injection of air, carbon dioxide and freon-12 are 0·85; 0·98; 1·14, respectively.

In [21] it is shown that for a non-isothermal boundary layer with longitudinal pressure gradient on an impenetrable surface form parameters ζ and H are functions of Γ. Therefore the expression $1\cdot 25[\zeta - (H + 1)\Gamma]$ is also a function of Γ

$$F(\Gamma) = 1\cdot 25[(\zeta - (H + 1)\Gamma]. \tag{44}$$

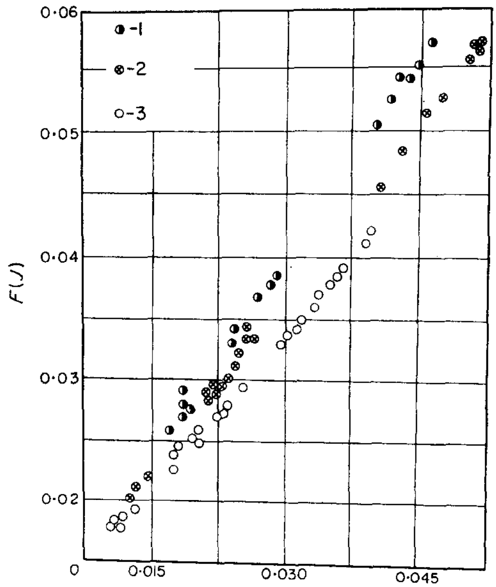

FIG. 6. Plot of $F(J)$ versus J.

The function $F(\Gamma)$ versus Γ is plotted as a straight line described by the following equation

$$F(\Gamma) = 0\cdot 016 - 3\cdot 55\Gamma. \tag{45}$$

Accounting for equations (43) and (45) one may write

$$F(\sigma) = 0\cdot 016 - 3\cdot 55\Gamma + mJ = 0\cdot 016 + m\sigma \tag{46}$$

where

$$\sigma = \frac{3\cdot 55}{m}\Gamma + J.$$

In Fig. 7 the function $F(\sigma)$ is plotted versus σ for injection of various gases. Location of experimental points in Fig. 7 confirms that $F(\sigma)$ is a linear function.

When the change of the injection form parameter is given, equation (42) with the account for equation (46) is reduced to a first order equation relative to $Re_\theta^{1\cdot 25}$

$$\frac{\mathrm{d}}{\mathrm{d}\bar{x}}(Re_\theta^{1\cdot 25}) + 3\cdot 55\, Re^{1\cdot 25}\cdot\frac{1}{u_1}\frac{\mathrm{d}u_1}{\mathrm{d}\bar{x}} - (mJ + 0\cdot 016)Re_L. \tag{47}$$

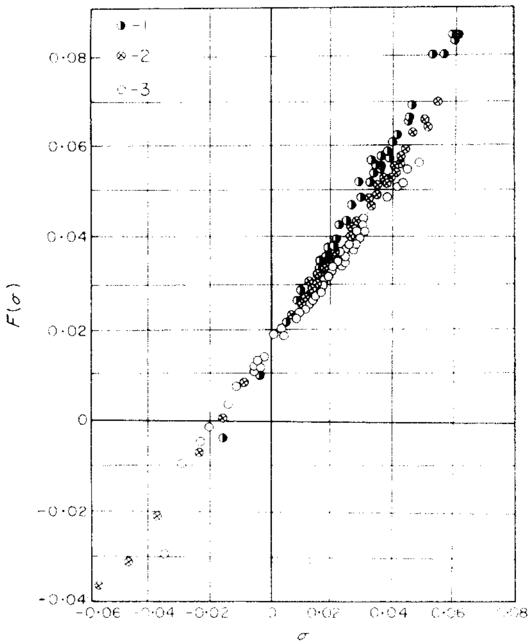

FIG. 7. Plot of $F(\sigma)$ versus σ.

The integral of equation (47) is equal to

$$Re_\theta = \{u_1^{-3\cdot 55}[\int_{\bar{x}_H}^{\bar{x}} (mJ + 0\cdot 016)Re_L \,.\, u^{3\cdot 55}\,\mathrm{d}x \quad C]\}^{0\cdot 8}. \qquad (48)$$

Here C is a constant of integration, $\bar{x}_H$ is the value of dimensionless co-ordinate at the starting point of the turbulent boundary layer under discussion.

$$C = \left[\frac{Re_\theta^{1\cdot 25} \,.\, u_1^{3\cdot 55}}{0\cdot 016}\right]_{\bar{x} = \bar{x}}$$

Thus, on the basis of data obtained, its interpretation and generalization, which allowed integration of the equation of motion, the following procedure may be recommended for estimating the dynamic boundary layer of a gas flow with longitudinal pressure gradient and transverse mass supply.

1. For given laws of velocity and temperature distribution of a non-disturbed flow, and also of the injection form parameter along the longitudinal co-ordinate x, the dependence of Re_θ (and consequently, θ) on x is determined from equation (48). If the relation $J(x)$ is not given but the law of mass supply of the gas being injected along the co-ordinates x when J is determined in equation (48), one may use the corresponding values of θ estimated from equation (30) of [21] for a turbulent boundary layer with longitudinal pressure gradient on an impenetrable surface.

Calculation shows that in this case errors in estimation of the thickness of momentum loss for the given conditions of flow are very small since Re_θ enters in J only as a power of 0·25.

2. From equations (31) and (41) values of the form parameters Γ and K are calculated as a function of x. In the case when the law of change of the form parameter $J(x)$ is not given, and in the integrand of equation (48) its value is estimated from the thickness of momentum loss under the approximate conditions on an impenetrable surface, finite values of J are computed from equation (33) after determining θ from equation (48).

3. Values of the form parameter ζ are found from the plot in Fig. 5, and then the corresponding local values of the drag coefficient on the wall are obtained from equation (32), depending on x.

4. If analytical relation $u_1(x_1)$, $(\rho_w v_w)/(\rho_1 u_1)\ (x)$ are not given, equation (48) may be integrated numerically using one of the conventional methods.

In Fig. 8 the effect of the injection rate on the dimensionless heat transfer factor is shown when a porous plate with longitudinal pressure gradient is located in a stream of heated air. Experi-

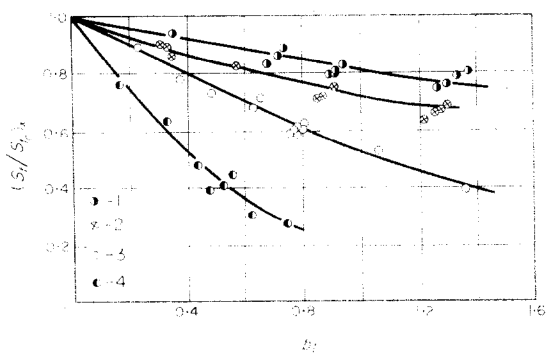

FIG. 8. Effect of injection rate of various gases on heat transfer coefficient at various values of b_T. Full lines denote appropriate relations for a flat plate.

mental points are plotted in this figure when helium, air, carbon dioxide and freon-12 are injected into an air flow with various values of the form parameter of the pressure gradient Γ. This figure shows that these data on St with change of Γ are actually the same as the values on a flat penetrable plate with appropriate values of the parameter b_T. Consequently, no effect of pressure gradient on heat transfer is manifest over the range of pressure gradient in our experiments. Friction drag on a porous plate decreases considerably with increase of longitudinal positive pressure gradient. As for a non-gradient flow, heat transfer on a surface in a gas stream may be reduced to a significant degree by increasing the quantity of injected gas, the actual consumption being relatively low.

The experimental dependence on Fig. 8 may be approximated by the equation

$$\frac{St}{St_o} = \exp(-a_T b_T). \tag{49}$$

Values of the constant a_T for injection of helium, air, carbon dioxide and freon-12 are 1·7; 0·64; 0·32; 0·2, respectively.

Using the equation (49) one may solve the integral energy relation.

Equation (12) may be written as follows

$$\frac{\mathrm{d}Re_\varphi}{\mathrm{d}\bar{x}} + \frac{Re_\varphi}{T_e - T_w}\frac{\mathrm{d}}{\mathrm{d}\bar{x}}(T_e - T_w) = Re_L\left(St + \frac{c_{pw}\rho_w v_w}{c_{p1}\rho_1 u_1}\right). \tag{50}$$

For the impenetrable flat plate is known the dependence

$$St_o = 0{\cdot}0128\, Re_\varphi^{-0\cdot25}\, Pr^{-0\cdot75}. \tag{51}$$

Taking into the account (49) and (51) from the equation (50), it follows

$$\frac{\mathrm{d}}{\mathrm{d}\bar{x}}(Re^{1\cdot25}) + 1{\cdot}25\frac{Re_\varphi^{1\cdot25}}{T_e - T_w}\frac{\mathrm{d}}{\mathrm{d}x}(T_e - T_w) = 0{\cdot}016\, Re_L\, Pr^{-0\cdot75}\,[b_T + \exp(-a_T b_T)]. \tag{52}$$

Accounting for $b_T = f(x)$ we obtain the integral of the equation (52)

$$Re_\varphi = \left\{\begin{array}{l}\dfrac{0{\cdot}016\, Re_{LH}}{Pr^{0\cdot75}(T_e - T_w)^{1\cdot25}}\displaystyle\int_{\bar{x}_H}^{\bar{x}} \bar{u}_1\,[b_T \\ \quad + \exp(-a_T b_T)]\,(T_e - T_w)^{1\cdot25}\,\mathrm{d}\bar{x} \\ \quad + \left[Re_\varphi^{1\cdot25}(T_e - T_w)^{1\cdot25}\right]_{\bar{x}_H}\end{array}\right\}^{0\cdot8} \tag{53}$$

where $\bar{u}_1 = (u_1/u_{1H})$ is the dimensionless velocity.

The obtained results may be used for definition of heat-transfer coefficient and the depth of energy loss, when $u_1(x)$; $b_T(x)$; $T_1(x)$; $T_w(x)$ are known.

REFERENCES

1. W. E. RANNIE, A simplified theory of porous wall cooling. Prog. Rept. 4–50, Power Plant. Lab, Proj. NMX 801, Jet Prop. Lab. CJT XI (1947).
2. H. S. MICKLEY, Heat, mass and momentum transfer for flow over a flat plate with blowing or suction. MIT, Cambridge, Mass. IX (1952).
3. W. H. DORRANCE and F. J. DORE, The effect of mass transfer on compressible turbulent boundary layer, skin-friction and heat transfer, *J. Aero. Space Sci.* **21**, 6, 404–410 (1954); **23**, 3, 283–284 (1956).
4. M. W. RUBESIN, An analytical estimation of the effect of transpiration cooling on the heat transfer and skin-friction characteristics of a compressible boundary layer. *NACA* TN 3341 (1956).
5. E. R. VAN DRIEST, On mass transfer near the stagnation point. RAND Symposium on mass transfer cooling for hypersonic flight (1957).
6. D. CLARKE, X. MENKS and P. A. LIBBY, A provisional analysis of turbulent boundary layer with injection, *J. Aero. Space Sci.* **22**, 4, 255–260 (1955).
7. L. E. KALIKHMAN, The turbulent boundary layer of an incompressible fluid on a porous plate (Turbulentnyi pogranichnyi sloi neszhimaemoi zhidkosti na poristoi stenke), *Zh. Tekh. Fiz.* **35**, 2, 1957–1964 (1955).
8. S. S. KUTATELADZE and A. I. LEONT'EV, The turbulent boundary layer of gas on a penetrable wall (Turbulentnyi pogranichnyi sloi gaza na pronitsaemoi stenke), *Prikl. Mat. Tekhn. Fiz.* No. 1, 51–60 (1962).
9. B. M. LEADON, Some experimental technique in mass transfer cooling, *Aero/Space Engng*, **18**, 10, 28–32 (1959).
10. H. S. MICKLEY and R. S. DAVIS, Momentum transfer for a flow over a flat plate with blowing. *NACA* TN 4017, XI (1957).
11. V. P. MUGALEV, Experimental investigation of the turbulent boundary layer on a plate with blowing of air and carbon dioxide in a supersonic flow (Eksperimental'noe izuchenie turbulentnogo pogranichnogo sloya na plastine pri vduvanii vozdukha i uglekislogo gaza v sverkhzvukovom potoke), *Trudy Mosk. Fiz.-Tekh. In-ta*, **4**, 152–171 (1959).
12. V. P. MUGALEV, An approximate method for calculation of friction and heat transfer with air injection

into a turbulent boundary layer (Priblizhennyi method rascheta treniya i teplootdachi pri vduvanii vozdukha v turbulentnom pogranichnom sloe), *Trudy Mosk. Fiz.-Tekh. In-ta*, **5**, 86–96 (1960).

13. D. S. HACKER, Empirical prediction of turbulent boundary layers instability along a flat plate with constant mass addition at the wall, *Jet Propulsion*, **26**, 9, 786–787 (1956).
14. C. C. PAPPAS and A. F. OKUNO, Measurements of skin-friction of the turbulent compressible layer on a cone with foreign gas injection, *J. Aero. Space Sci.* **27**, 5, 321–333 (1960).
15. J. P. HARTNETT, D. J. MASSON, J. F. GROSS and C. J. GAZLEY, Mass transfer cooling in a turbulent boundary layer, *J. Aero. Space Sci.* No. 8, 623–625 (1960).
16. A. I. TOLSTYKH, A turbulent boundary layer with pressure gradient on a porous plate (Turbulentnyi pogranichny sloi s gradientom gavleniya na poristoi poverkhnosti), *Inzh. Zhur.* **2**, 1, 79–85 (1962).
17. P. N. ROMANENKO and A. I. LEONT'EV, Experimental investigation of a turbulent boundary layer with gas motion in axi-symmetrical diffusers with the refrigerated walls (Eksperimental'noe issledovanie turbulentnogo pogranichnogo sloya pri dvizhenii gaza v osesimmetrichnykh diffuzorakh s okhlazhdaemymi stenkami), *Trudy Mosk. In-ta Inzh. Zhel.-Dor. Transporta* **139**, 134–157 (1961).
18. E. R. G. ECKERT and R. M. DRAKE, *Heat and Mass Transfer*. McGraw-Hill, New York (1959).
19. F. H. CLAUSER, Turbulent boundary layer in adverse pressure gradient, *J. Aero. Space Sci.* **21**, 2, 91–108 (1954).
20. H. SCHLICHTING, *Grenzschicht-Theorie*, Karlsruhe (1951).
21. P. N. ROMANENKO, A. I. LEONT'EV and A. N. OBLIVIN, Investigation on resistance and heat transfer of a turbulent air flow in axisymmetrical channels with longitudinal pressure gradient, *Int. J. Heat Mass Transfer*, **5**, 541–557 (1962).

Abstract—Experimental investigations were carried out on the friction drag and heat transfer of a porous surface in a heated air flow at $dp/dx = 0$ and $dp/dx \neq 0$ with the injection of various gases (helium, air, carbon dioxide and freon-12). The effect of relative flow of injected gases on a flat plate and of longitudinal pressure gradient (the case $dp/dx \neq 0$) on heat transfer and friction drag is found. It is shown that with increase of molecular weight of injected gases, their effect on heat transfer and friction drag decreases. Longitudinal pressure gradient considerably influences friction drag rather strongly, but it has no effect on heat transfer rate.

Experimental data and their correlation by relations between dimensionless parameters of friction, pressure gradient and injection allowed the relation between the main characteristic quantities for a turbulent boundary layer to be evaluated under conditions of heat and mass transfer and longitudinal pressure gradient.

Résumé—Les auteurs ont étudié expérimentalement le frottement et la transmission de chaleur sur une surface poreuse placée dans un écoulement d'air chaud, dans les cas où $dp/dx = 0$ et $dp/dx \neq 0$, avec injection de différents gaz (hélium, air, gaz carbonique et Fréon 12). L'effet de l'écoulement injecté et du gradient de pression ($dp/dx \neq 0$) sur la transmission de chaleur et le frottement a été mis en évidence. Cet effet diminue lorsque le poids moléculaire des gaz injectés augmente. Le gradient longitudinal de pression a une grosse influence sur le frottement mais aucune sur le coefficient d'échange thermique.

Les données expérimentales et leur corrélation, traduite sous forme d'expressions liant les paramètres de frottement, de gradient de pression et d'injection, ont permis d'établir une relation entre les grandeurs caractéristiques principales de la couche limite turbulente avec transport de masse et de chaleur et gradient de pression longitudinal.

Zusammenfassung—In einem warmen Luftstrom wurde der Reibungswiderstand und der Wärmeübergang an einer porösen Oberfläche bei Einblasung verschiedener Gase (Helium, Luft, Kohlendioxyd und Freon 12) und $dp/dx = 0$ und $dp'/dx \neq 0$ experimentell untersucht. Der Einfluss des Relativstroms der eingeblasenen Gase an der ebenen Platte und des Längsdruckgradienten (Fall $dp/dx \neq 0$) auf Wärmeübergang und Reibungswiderstand liess sich ermitteln. Es zeigt sich, dass mit ansteigendem Molekulargewicht der Einblasgase, ihr Einfluss auf Wärmeübergang und Reibungswiderstand abnimmt. Ein Druckgradient in Längsrichtung beeinflusst den Reibungswiderstand sehr stark, nicht jedoch den Wärmeübergang.

Die Versuchsdaten und Korrelationen zwischen dimensionslosen Reibungsparametern, dem Druckgradienten und Einblaswerten, gestatteten die Berechnung der charakteristischen Grössen für turbulente Grenzschichten bei gleichzeitiger Wärme- und Stoffübertragung unter einem Längsdruckgradienten.